# PART 2

# LM3-EUTRO

## Chapter 5. Calibration

### *2.5.1 Description of Process*

After model equations were formulated and coded as a computer program, model calibration was the next step. The goal of calibrating water quality models was to adjust the model coefficients in order to obtain the best possible fit between the model output and the field data. Challenges of calibrating eutrophication models included the many degrees of freedom (independent model coefficients) and the uncertainty of many of these model coefficients. A traditional model calibration approach was used for LM3-Eutro. The model coefficients were initially estimated using values and ranges reported in the literature (see Table 2.4.7) and these parameters were then adjusted to provide the best model fit to the field data. In this study, values for many coefficients were derived from available Lake Michigan and Great Lakes historical data collected by reputable agencies such as the United States Environmental Protection Agency's (USEPA) Great Lakes National Program Office (GLNPO), National Oceanic and Atmospheric Administration's (NOAA) Great Lakes Environmental Research Laboratory (GLERL) and the University of Michigan. Very few field and laboratory experiments were performed to estimate kinetic coefficients for LM3-Eutro. Limited $^{14}C$ primary production experiments were performed and used in determining phytoplankton growth coefficients. Phytoplankton (diatoms and non-diatoms), particulate organic carbon (POC), total phosphorus, and dissolved silica (DSi) were the most important state variables in model calibration. However, all variables were evaluated during the calibration process.

The model was calibrated on the Level 3 segmentation framework (Figure 2.5.1). The main calibration emphasis was placed on the main lake due to inadequate Green Bay data. The high-resolution (Level 3) segments were also collapsed to the Level 2 segmentation scheme to provide a visual representation of how well the model reflected the field data in different areas of the lake and captured expected trends, such as spring epilimnetic diatom peaks and nutrient depletion. It was not

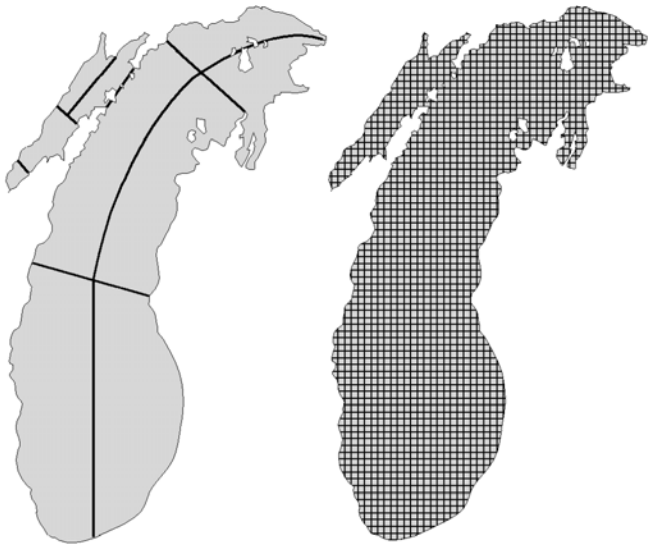


**Figure 2.5.1. Level 2 and Level 3 model segmentation.**

feasible to visually compare model output versus field data on the Level 3 segmentation framework due to the large number (44,042) of 5 $km^2$ cells. Instead, we regressed model output versus field data for each of the 5 $km^2$ cells where a field data point was available. This enabled calculation of simple statistical parameters such as square of the correlation coefficient ($r^2$) and slope and direct comparison of the different model calibration runs.

During the calibration process, small changes to the model initial conditions were made to observe the effect on the model fit. This was done because of the uncertainty of the initial condition estimates and the fact that the initial conditions have a significant influence on the model output.

Data from laboratory primary productivity experiments were used to constrain and confirm values for the growth coefficients that were used in the model. Productivity experiment results; light and temperature parameters; and the Lake Michigan Mass Balance Project (LMMBP) field data were applied to LM3-Eutro productivity equations to generate model production estimates comparable to those generated in the laboratory experiments. Model constants were then adjusted in order to best reflect the primary production trends observed in the laboratory experiments (Figure 2.5.2).

## *2.5.2 Selection of Best Calibration*

After performing several hundred model simulations, we selected our best run based on statistical parameters including square of correlation coefficient ($r^2$) and slope. The coefficients of the final run were constrained to ensure that all model coefficients fell within reasonable and reported ranges. The best model fit was also evaluated visually on the Level 2 segmentation scheme. Important criteria included the model fit with the overall field data, ability to capture observed and expected phytoplankton peaks, and how well hypolimnetic and epilimnetic nutrient, carbon, and plankton trends and concentrations were predicted. The calibrated final model coefficients are listed in Table 2.5.1. Figure 2.5.3 shows the overall Level 3 fit for phytoplankton, total phosphorus, POC, and DSi. Statistical results are summarized in Table 2.5.2. Figure 2.5.4 shows model versus field data plots for selected Level 2 segments. Selected Level 3 5 $km^2$ cells representing nearshore regions and offshore regions are presented in Figure 2.5.5. Model output for the 5 $km^2$ cells was much more dynamic than for the larger Level 2 segments and there were far fewer data points for model fit determination. The model appeared to fit the available data very well in some of the cells and not as well in others. Level 3 model versus data comparisons in individual 5 $km^2$ cells were not used in our calibration exercise.

Although we attempted to calibrate all of the state variables, less emphasis was placed on the nitrogen states because Lake Michigan is phosphorus and silica-limited. We also did not perform any comparison of model output with the field data for particulate silica (SU) or soluble reactive phosphorus (SRP), since there was no SU field data and more than 80% of the SRP field data fell below the detection limit. As stated, we did not spend much time calibrating Green Bay because of the limited sampling done in the bay. As a consequence, the final Green Bay calibration was not as good as the rest of the lake. This was especially true for the portion of the bay closest to the Fox River.

With the exception of zooplankton, the final model calibration was reasonably good, and the model was able to fit the field data well and capture important spatial and seasonal trends. A brief discussion of individual calibration results for phytoplankton, POC, total phosphorus, and DSi follows.

### 2.5.2.1 Phytoplankton

The model somewhat underestimated the field data for phytoplankton. Seabird chlorophyll *a* data were used for all phytoplankton field values. Part of the explanation for the underestimation was poor chlorophyll *a* field data. The Seabird fluorescence instrument, like many *in vivo* fluorescence methods, is notorious for its inaccuracy in measuring chlorophyll *a* (U.S. Environmental Protection Agency, 1997; Clesceri *et al*., 1998). The square of the correlation coefficient of 0.37 was acceptable, especially given the inherent variation in phytoplankton communities over space and time. Our fit was in-range of other published eutrophication models (Thomann, 1982; Cerco and Cole, 1994). The model was able to capture spatial and temporal trends such as the spring diatom blooms (Figure 2.5.4) and earlier phytoplankton blooms in the

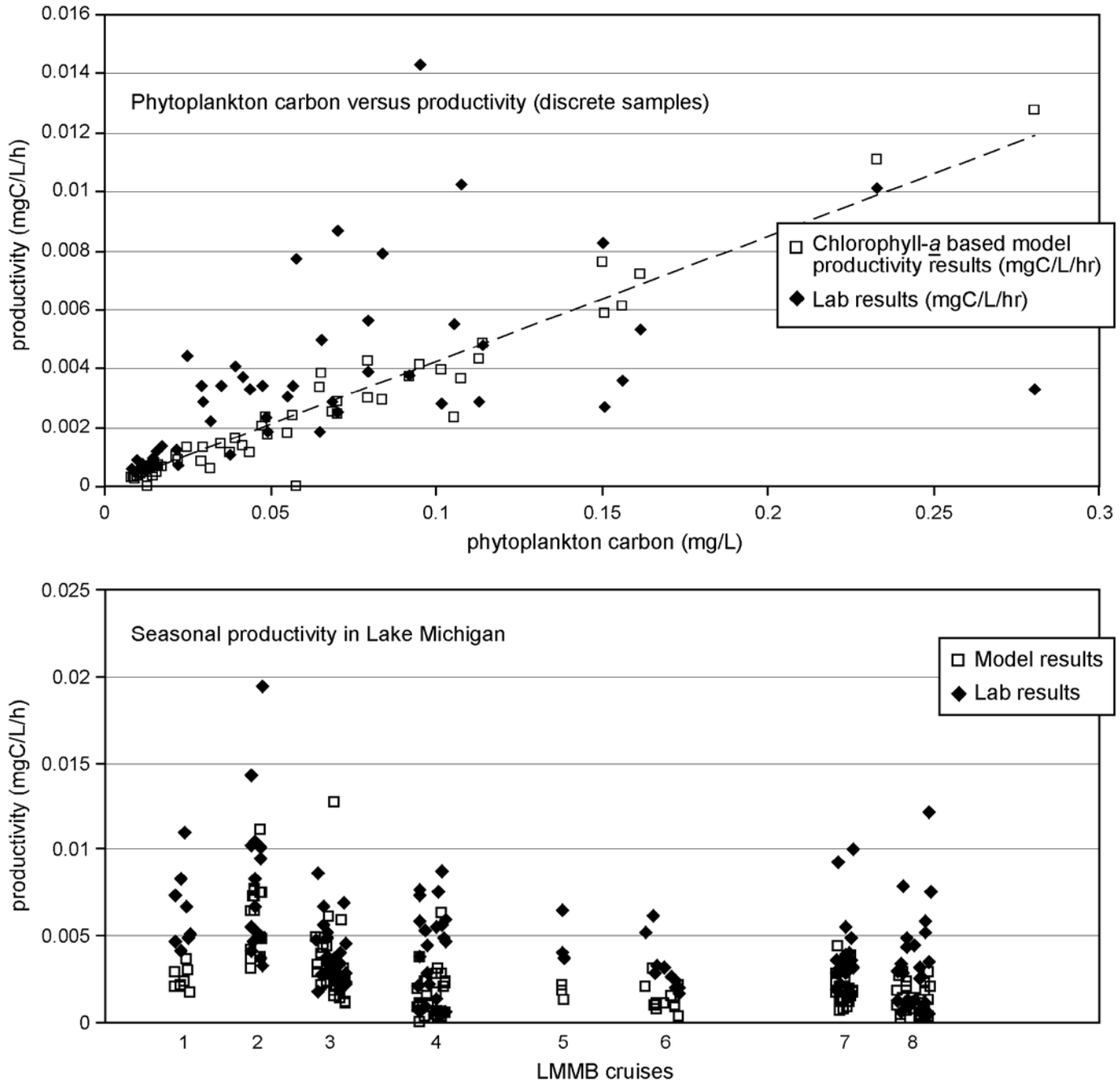


**Figure 2.5.2. LM3-Eutro model versus laboratory primary production.**

**Table 2.5.1. Coefficients Used in the LM3 Model (Units Correspond to Required LM3 Model Output)**

| Coefficient | Value | Unit | Description |
|---|---|---|---|
| ANCP | 0.25 | | Nitrogen:carbon ratio (mass basis) |
| APCP | 0.01 | | Phosphorus:carbon ratio (mass basis) |
| ASCD | 2.3 | | Silica:carbon ratio (mass basis) |
| BMRD | 8.6E-07 | 1/s | Diatom mortality |
| BMRG | 8.6E-07 | 1/s | Greens mortality |
| CCHLD | 40 | | Carbon:chlorophyll ratio (diatoms) |
| CCHLG | 40 | | Carbon:chlorophyll ratio (greens) |
| CGZ | 3.1E-06 | $m^3/kg/s$ | Zooplankton grazing rate coefficient |
| FCDD | 0.05 | | Dissolved organic carbon fraction from diatom mortality |
| FCDG | 0.05 | | Dissolved organic carbon fraction from greens mortality |
| FCLD | 0.3 | | Labile organic carbon fraction from diatom mortality |
| FCLG | 0.3 | | Labile organic carbon fraction from greens mortality |
| FCRD | 0.3 | | Refractory organic carbon fraction from diatom mortality |
| FCRG | 0.3 | | Refractory organic carbon fraction from greens mortality |
| FCDP | 0.35 | | Dissolved organic carbon fraction from algal predation |
| FCDZ | 0 | | Dissolved organic carbon fraction from zooplankton mortality |
| FCLP | 0.5 | | Labile particulate dissolved carbon fraction from algal predation |
| FCLZ | 0.4 | | Labile particulate dissolved carbon fraction from zooplankton mortality |
| FCRP | 0.15 | | Refractory particulate dissolved carbon fraction from algal predation |
| FCRZ | 0.1 | | Refractory particulate dissolved carbon from zooplankton mortality |
| FNDD | 0.5 | | Dissolved organic nitrogen from diatom mortality |
| FNDG | 0.5 | | Dissolved organic nitrogen fraction from greens mortality |
| FNDP | 0 | | Dissolved organic nitrogen fraction from algal predation |
| FNDZ | 0 | | Dissolved organic nitrogen fraction from zooplankton mortality |
| FNID | 0.5 | | Dissolved inorganic nitrogen fraction from diatom mortality |
| FNIG | 0.5 | | Dissolved inorganic nitrogen fraction from greens mortality |
| FNIP | 0.5 | | Dissolved inorganic nitrogen fraction from algal predation |
| FNIZ | 0.5 | | Dissolved inorganic nitrogen fraction from zooplankton mortality |
| FNLD | 0 | | Labile organic nitrogen fraction from diatom mortality |
| FNLG | 0 | | Labile organic nitrogen fraction from greens mortality |
| FNLP | 0.4 | | Labile organic nitrogen fraction from algal predation |
| FNLZ | 0.4 | | Labile organic nitrogen fraction from zooplankton mortality |
| FNRD | 0 | | Refractory organic nitrogen fraction from diatom mortality |
| FNRG | 0 | | Refractory organic nitrogen fraction from greens mortality |
| RNRP | 0.1 | | Refractory organic nitrogen fraction from algal predation |
| RNRZ | 0.1 | | Refractory organic nitrogen fraction from zooplankton mortality |
| FPDD | 0.1 | | Dissolved organic phosphorus fraction from diatom mortality |
| FPDG | 0.1 | | Dissolved organic phosphorus fraction from greens mortality |
| FPDP | 0.2 | | Dissolved organic phosphorus fraction from algal predation |
| FPDZ | 0.2 | | Dissolved organic phosphorus fraction from zooplankton mortality |
| FPID | 0.3 | | Dissolved inorganic phosphorus fraction from diatom mortality |
| FPIG | 0.3 | | Dissolved inorganic phosphorus fraction from greens mortality |
| FPIP | 0.5 | | Dissolved inorganic phosphorus fraction from algal predation |
| FPLD | 0.5 | | Dissolved inorganic phosphorus fraction from zooplankton mortality |
| FPLG | 0.3 | | Labile organic phosphorus fraction from greens mortality |
| FPLP | 0.15 | | Labile organic phosphorus fraction from algal predation |
| FPLZ | 0.15 | | Labile organic phosphorus fraction from zooplankton mortality |
| FPRD | 0.3 | | Refractory organic phosphorus fraction from diatom mortality |
| FPRG | 0.3 | | Refractory organic phosphorus fraction from greens mortality |
| FPRP | 0.15 | | Refractory organic phosphorus fraction from algal predation |
| FPRZ | 0.15 | | Refractory organic phosphorus fraction from zooplankton mortality |

**Table 2.5.1. Coefficients Used in the LM3 Model (Continued)**

| Coefficient | Value | Units | Description |
|---|---|---|---|
| FSAP | 0 | | Dissolved silica fraction from diatom predation |
| GREFF | 0.6 | | Zooplankton grazing coefficient |
| ILUMO | 25 | $W/m^2$ | Constant illumination (first 90 days) |
| ISMIN | 400 | $W/m^2$ | Optimum light illumination |
| KDC | 1.16E-08 | 1/s | Dissolved organic carbon mineralization coefficient |
| KDCALG | 0.00E+00 | $m^3/kg/s$ | Dissolved organic carbon algal dependency coefficient |
| KDN | 1.74E-07 | 1/s | Dissolved organic nitrogen mineralization coefficient |
| KDNALG | 0.00E+00 | $m^3/kg/s$ | Dissolved organic nitrogen algal dependency coefficient |
| KDP | 1.16E-09 | 1/s | Dissolved organic phosphorus mineralization coefficient |
| KDPALG | 6.0E-03 | $m^3/kg/s$ | Dissolved organic phosphorus algal dependency coefficient |
| KE | 0.15 | 1/m | Background light attenuation |
| KECHL | 1.7E+04 | $m^2/kg$ | Light attenuation for chlorophyll *a* |
| KHND | 2.50E-05 | $kg/m^3$ | Nitrogen half-saturation coefficients for diatoms |
| KHNG | 2.50E-05 | $kg/m^3$ | Nitrogen half-saturation coefficients for greens |
| KHNNT | 0.0000 | $kg/m^3$ | Nitrate half-saturation coefficient for nitrification |
| KHPD | 5.0E-07 | $kg/m^3$ | Phosphorus half-saturation coefficients for diatoms |
| KHPG | 5.0E-07 | $kg/m^3$ | Phosphorus half-saturation coefficients for greens |
| KHSD | 6.0E-05 | $kg/m^3$ | Silica half-saturation coefficients for diatoms |
| KLC | 1.0E-07 | 1/s | Labile organic carbon hydrolysis coefficient |
| KLCALG | 0.00E+00 | $m^3/kg/s$ | Labile organic carbon algal dependency coefficient |
| KLN | 3.47E-07 | 1/s | Labile organic carbon hydrolysis coefficient |
| KLNALG | 0.00E+00 | $m^3/kg/s$ | Labile organic nitrogen algal dependency coefficient |
| KLP | 1.00E-09 | 1/s | Labile organic phosphorus hydrolysis coefficient |
| KLPALG | 6.00E-03 | $m^3/kg/s$ | Labile organic phosphorus algal dependency coefficient |
| KRC | 1.00E--07 | 1/s | Refractory organic carbon hydrolysis coefficient |
| KRCALG | 0.00E+00 | $m^3/kg/s$ | Refractory organic carbon algal dependency coefficient |
| KRN | 3.47E-08 | 1/s | Refractory organic nitrogen hydrolysis coefficient |
| KRNALG | 00E+00 | $m^3/kg/s$ | Refractory organic nitrogen algal dependency coefficient |
| KRP | 1.0E-09 | 1/s | Refractory organic phosphorus hydrolysis coefficient |
| KRPALG | 6.0E+03 | $m^3/kg/s$ | Refractory organic phosphorus algal dependency coefficient |
| KSUA | 2.5E-07 | 1/s | Biogenic silica dissolution rate |
| KSZ | 1.0E-04 | $kg/m^3$ | Zooplankton half-saturation (for algae) |
| KTBD | 0.074 | 1/°C | Diatom mortality temperature coefficient |
| KTBG | 0.074 | 1/°C | Greens mortality temperature coefficient |
| KTGD1 | 0.0025 | $1/°C^2$ | Diatom growth temperature coefficient (< optimum) |
| KTGD2 | 0.006 | $1/°C^2$ | Diatom growth temperature coefficient (> optimum) |
| KTGG1 | 0.0025 | $1/°C^2$ | Greens growth temperature coefficient (< optimum) |
| KTGG2 | 0.006 | $1/°C^2$ | Greens growth temperature coefficient (> optimum) |
| KTHDR | 9.9E-02 | 1/°C | Hydrolysis temperature dependency coefficient |
| KTMNL | 7.4E-02 | 1/°C | Mineralization temperature dependency coefficient |
| KTNT1 | 0.004 | $1/°C^2$ | Nitrification temperature coefficient (< optimum) |
| NTNT2 | 0.004 | $1/°C^2$ | Nitrification temperature coefficient (> optimum) |
| KTSUA | 0.069 | 1/°C | Silica dissolution temperature coefficient |
| NTM | 0.074 | 1/°C | Diatom mortality temperature coefficient |
| NTM | 2.50E-11 | $kg/m^3/s$ | Nitrification rate coefficient |
| PMD | 2.90E-05 | 1/s | Diatom growth coefficient |
| PMG | 2.60E-05 | 1/s | Greens growth coefficient |
| TMD | 18 | °C | Optimum diatom growth temperature |
| TMG | 18 | °C | Optimum greens growth temperature |
| TMNT | 30 | °C | Optimum nitrification temperature |
| TRD | 20 | °C | Optimum diatom mortality temperature |

**Table 2.5.1. Coefficients Used in the LM3 Model (Continued)**

| Coefficient | Value | Units | Description |
|---|---|---|---|
| TRG | 20 | °C | Optimum greens mortality temperature |
| TRHDR | 20 | °C | Optimum hydrolysis temperature |
| TRMNL | 20 | °C | Optimum mineralization temperature |
| TRSUA | 20 | °C | Optimum silica dissolution temperature |
| TZREF | 20 | °C | Optimum predation temperature |
| ZDTH | 5.0E-07 | 1/s | Zooplankton mortality rate coefficient |
| ZTHET | 1.0 | | Arrhenius temperature coefficient for predation |
| VDIA | 1.15E-06 | m/s | Diatoms settling coefficient |
| VGRE | 0.85E-06 | m/s | Greens settling coefficient |
| VLOC | 2.0E-06 | m/s | Labile organic carbon settling coefficient |
| VROC | 2.0E-06 | m/s | Refractory organic carbon settling coefficient |
| VLON | 2.0E-06 | m/s | Labile organic nitrogen settling coefficient |
| VRON | 2.0E-06 | m/s | Refractory organic nitrogen settling coefficient |
| VLOP | 2.0E-06 | m/s | Labile organic phosphorus settling coefficient |
| VROP | 2.0E-06 | m/s | Refractory organic phosphorus settling coefficient |
| VSU | 2.0E-06 | m/s | Biogenic silica settling coefficient |

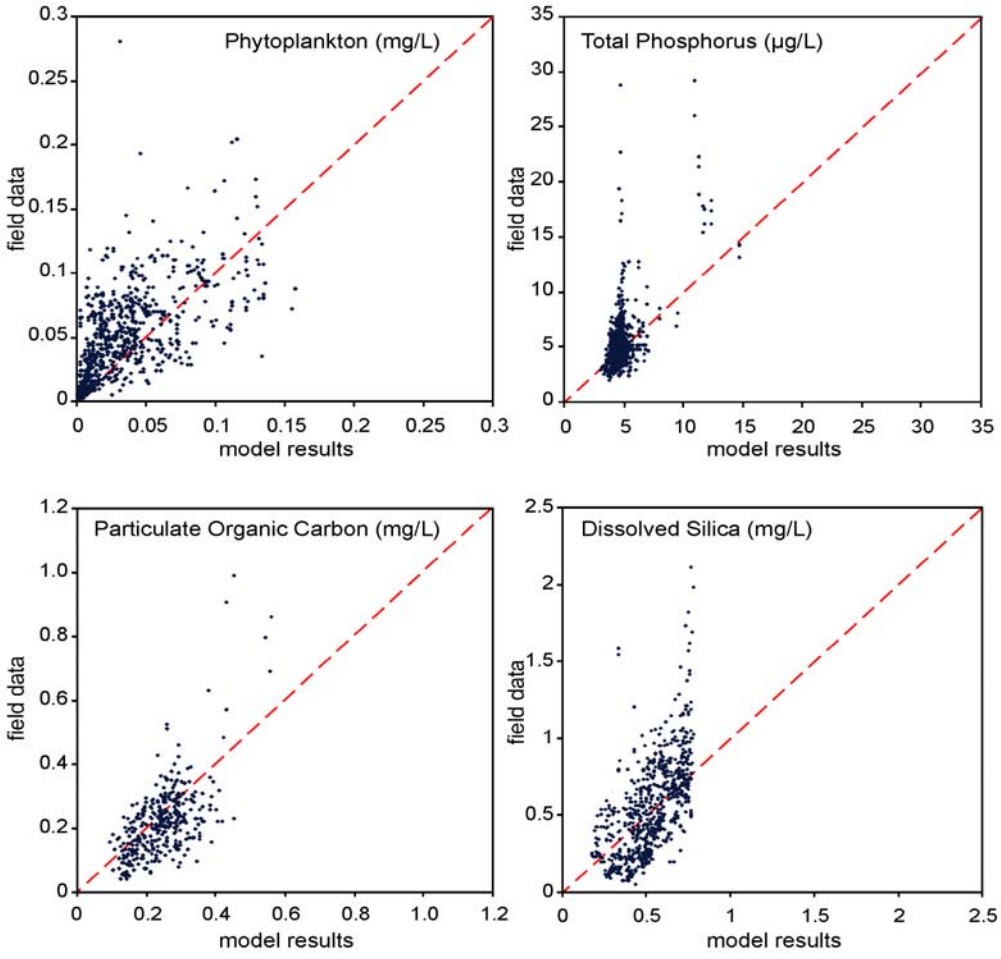


**Figure 2.5.3. Level 3 LM3-Eutro model predictions versus field data, lake-wide.**

**Table 2.5.2. Summary of Statistical Results of the Calibration**

| Variable | Regression Coefficient ($r^2$) | Slope |
|---|---|---|
| Phytoplankton | 0.37 | 0.67 |
| Particulate Organic Carbon | 0.39 | 0.95 |
| Total Phosphorus | 0.37 | 1.4 |
| Dissolved Silica | 0.37 | 1.2 |
| Zooplankton | 0.13 | 0.43 |

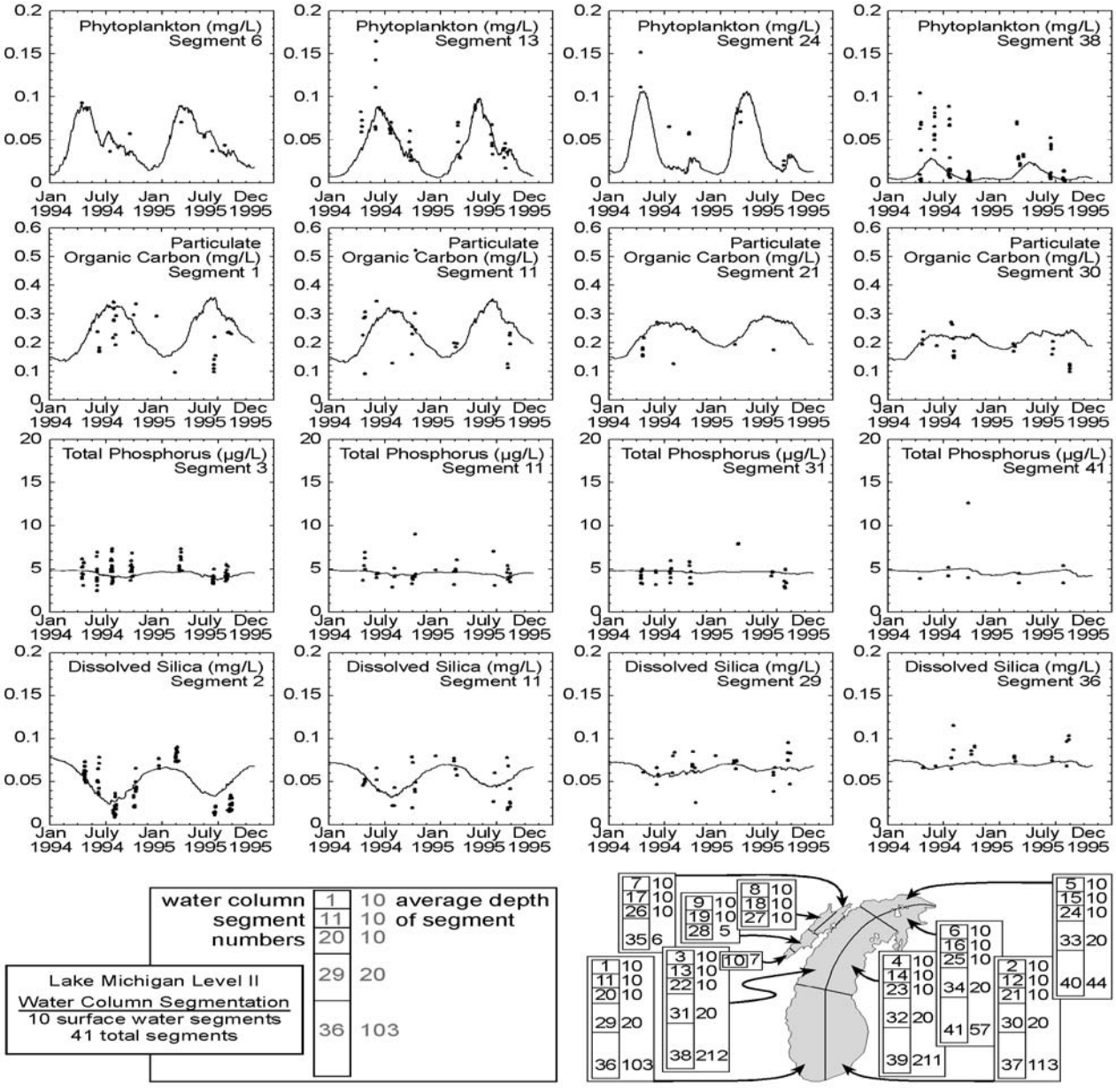


**Figure 2.5.4. Level 2 LM3-Eutro model output versus field data for selected segments.**

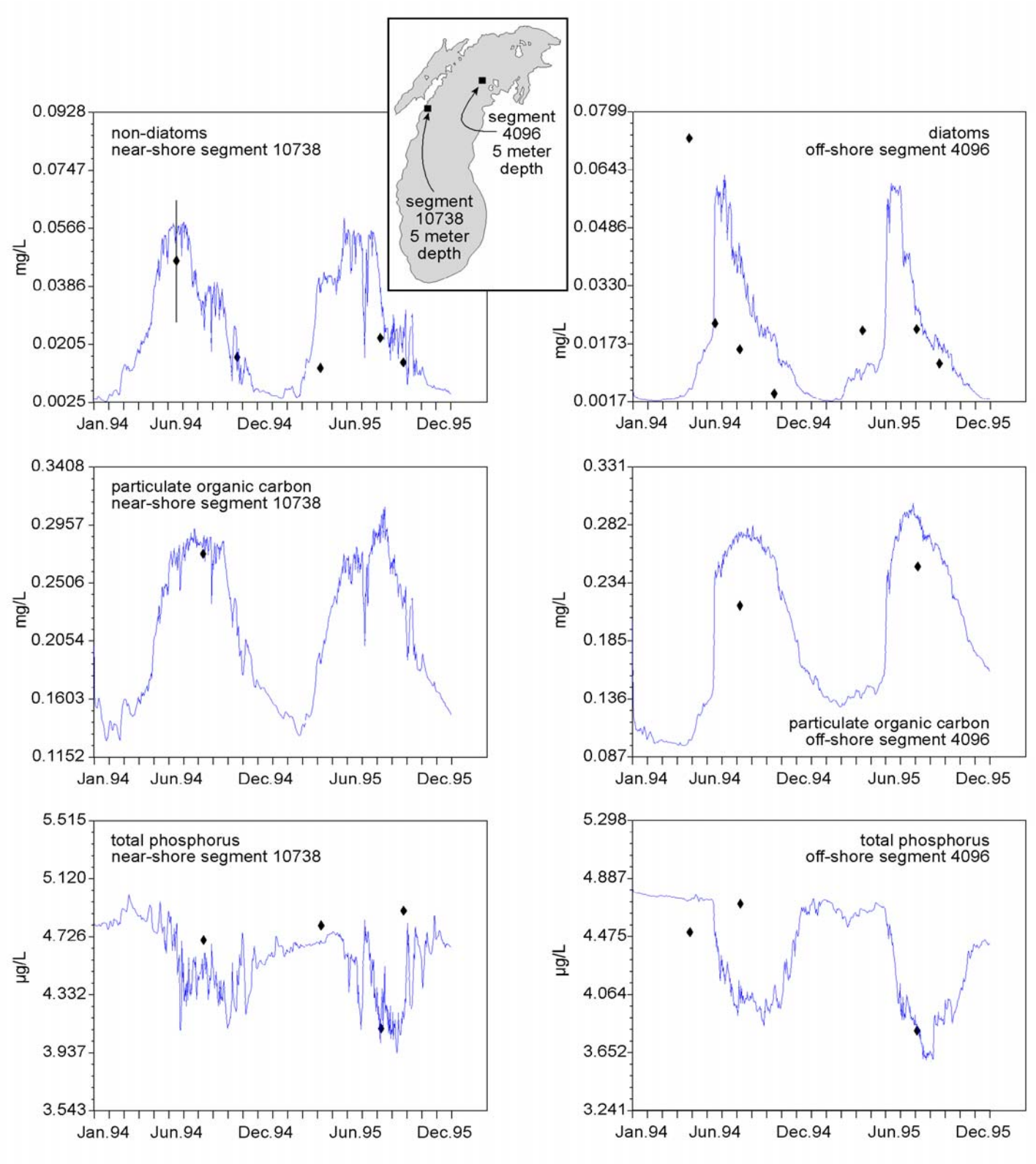


**Figure 2.5.5. Level 3 LM3-Eutro model output versus field data for selected nearshore and offshore cells.**

nearshore cells than in the offshore cells (Figure 2.5.5).

#### 2.5.2.2 Particulate Organic Carbon

The model fits the field data well (Figure 2.5.3), with a slope of almost one (0.95) and a square of the correlation coefficient of almost 0.4 ($r^2 = 0.39$). The POC data exhibited less scatter than the other variables and were reflective of the phytoplankton in the lake. Additionally, we had a great deal of confidence in the POC data measurement technique. The ability of the model to capture the POC data trend increased our confidence in the model's overall eutrophication predictions. Examination of Level 2 segments showed that the model captured important trends, such as higher POC concentrations during the spring diatom bloom (Figure 2.5.4).

#### 2.5.2.3 Total Phosphorus

The model fits the total phosphorus data reasonably well with a slope of 1.4 and a square of the correlation coefficient of 0.37. In general, the total phosphorus concentrations in the lake were fairly constant, with most measurements falling between 4 and 5 µg/L and little seasonal variation observed. The overall model fit was acceptable (Figure 2.5.4). However, there were several higher total phosphorus values measured in Green Bay close to the Fox River and at other nearshore stations close to rivers and/or areas where there were significant sediment resuspension. In these cases, the model was not able to mimic the data, probably due to initial conditions that were too low and the lack of a sediment resuspension term.

#### 2.5.2.4 Dissolved Silica

The dissolved silica model fits the field data well, with a slope of 1.2 (influenced by several very high silica field data points) and a regression coefficient of 0.37. The model predicted the expected trends, with highest silica in the winter, a steep decline in the epilimnion in the spring coinciding with the diatom bloom, and a recovery toward the end of the year (Figure 2.5.4).

In general, the model fit the field data reasonably well. Seasonal and spatial trends for important variables, such as phytoplankton and silica, were captured. There were difficulties in accurately predicting Green Bay phytoplankton and nutrient concentrations, but this was not unexpected.

## References


Cerco, C. and T. Cole. 1994. Three-Dimensional Eutrophication Model of Chesapeake Bay. U.S. Army Corps of Engineers, U.S. Army Engineer Waterways Experiment Station, Vicksburg, Mississippi. Technical Report Number EL-94-4, 658 pp.

Clesceri, L.S., A.E. Greenberg, and A.D. Eaton (Eds.). 1998. Standard Methods for the Examination of Water and Wastewater, 20th Edition. American Public Health Association, American Water Works Association, and Water Environment Federation, Hanover, Maryland. 1,205 pp.

Thomann, R.V. 1982. Verification of Water Quality Models. J. Environ. Engin., 108(EE5):933-940.

U.S. Environmental Protection Agency. 1997. Lake Michigan Mass Balance Study (LMMB) Methods Compendium, Volume 1: Sample Collection Techniques. U.S. Environmental Protection Agency, Great Lakes National Program Office, Chicago, Illinois. EPA/905/R-97/012a, 1,440 pp.